Modeling the dual role of SIRT1 in p53-dependent mitochondrial apoptosis

Nan Liu
Inner Mongolia University
Hongli Yang (imuyhl@imu.edu.cn)
Inner Mongolia University https://orcid.org/0000-0002-5060-4748
Liangui Yang
Inner Mongolia University

Research

Keywords: SIRT1, p53, BCL-2 protein family, Apoptosis

Posted Date: May 4th, 2021

DOI: https://doi.org/10.21203/rs.3.rs-470662/v1

RESEARCH

Modeling the dual role of SIRT1 in p53-dependent mitochondrial apoptosis

Nan Liu, Hongli Yang* and Liangui Yang

*Correspondence:
imuyhl@imu.edu.cn
School of Mathematical Sciences, Inner Mongolia University, Hohhot 010021, China
Full list of author information is available at the end of the article

Abstract

Apoptosis, or called programmed cell death, is an inherent protective mechanism in the body. Mitochondrial apoptosis is inseparable from BCL-2 protein family. The tumor suppressor protein p53 can prevent the proliferation of cells with abnormal genetic information (including cancer cells) by regulating apoptosis. It has been reported that SIRT1 has an effect on p53-mediated apoptosis, theoretical models in this regard, however, are still scarce. Therefore, this work developed a mathematical model to simulate the roles of SIRT1 in p53-mediated apoptosis. We first investigated the apoptosis of this gene network under three stress modes. Then, the method of bifurcation analysis was used. In agreement with the experimental reports, the model showed that there is an optimal content of SIRT1, at which the cell's apoptotic ability is strongest. This paper provided new insights about the SIRT1-p53 axis in tumorigenesis, and may be useful for clinical treatment.

Keywords: SIRT1; p53; BCL-2 protein family; Apoptosis

Background

Apoptosis, also known as programmed cell death, is a physiological process that approves cell suicide. It is apoptosis that forces the damaged, the infected or transformed abnormal cells are eliminated by themselves, and failure to trigger apoptosis will increase the probability of tumor occurrence [1]. Therefore, apoptosis is indispensable to the healthy growth of living organisms. In biotechnology applications, apoptosis can be triggered by chemotherapy drugs, radiation, or the withdrawal of growth factors. One of the characteristics of these apoptotic cells is the permeability of the outer mitochondrial membrane and the release of cytochrome C into the cytoplasm [2]. In this process, the signal network formed by the mutual regulation of the BCL-2 protein family played a dominant role [3]. According to functions, BCL-2 protein family can be divided into three categories: i) directly promote mitochondrial apoptosis pathway species, such as Bax; ii) species that inhibit apoptosis, such as Bcl-2; iii) indirectly promote apoptosis species, i.e. Bh3-only proteins, such as Puma [4].

A well-known tumor suppressor transcription factor, p53, is also involved in the BCL-2 signaling protein network in indirect and direct ways. In the indirect route, it has been verified that the acetylation of p53 in the nucleus is crucial for a Bh3-only protein Puma's induction [5]; In the direct route, it has been unraveled that p53 in the cytoplasm forming a complex with Bcl-2 is a novel mechanism to anti-tumor [6]. Through mathematical modeling studies, Pu et al proposed that the

balance of p53 content in the cytoplasm and nucleus is required for reliable cell fate decisions [7]. Latter, Tian et al used the mathematical model that p53 directly and indirectly participates in the biochemical reaction of BCL-2 family proteins to ingeniously explain the experimental phenomenon of two waves apoptosis in mouse cells under DNA damage [8]. Although there have been theoretical models discussing that nuclear p53 transactivates pro-apoptotic genes and cytoplasmic p53 induces mitochondrial-dependent apoptosis without gene transactivation, SIRT1 also affects p53 translocation and transcriptional activity [9], there is little theoretical work thinking about how SIRT1 affects cell fate.

Based on the above considerations, we developed a new mathematical model of the crosstalk between the p53 module and the BCL-2 protein family module to explore the function of SIRT1 on apoptosis, where the BCL-2 protein family module comes from Ref. [10]. Through numerical simulations, we revealed that multiple stress modes all have the potential to trigger programmed cell death, and the cooperation of p53 in the nucleus and cytoplasm plays a key role in apoptosis. Next, we reduced or enlarged the SIRT1 generation rate to watch the evolution of apoptotic protein levels over time under various pressures, and found that an increase or decrease in the concentration of SIRT1 all may cause the initiation of apoptosis to be delayed. Finally, we used the numerical bifurcation method to analyze the system dynamics under the co-regulation of pressure and SIRT1, and reinterpreted that the SITR1 generation rate to an appropriate value is the best for cancer prevention. We highlight the dual role of SIRT1 in apoptosis (anti-cancer), and this result is supported by some previous experimental observations [11]. This work supplied a theoretical framework for artificially intervening the p53-SIRT1 axis to treat cancer cells.

Theoretical model

The model we considered is shown in Fig.1. It is assumed that stress activates the transcriptional activity of p53 and promotes the rapid degradation of Mdm2 in the nucleus [12, 13]. Unmodified p53 can enter and exit the nucleus freely, unlike activated (phosphorylated and acetylated) p53 that is confined in the nucleus [14]; Mdm2 is phosphorylated before it can shuttle through the nuclear membrane, while unmodified Mdm2 is isolated in the cytoplasm [15]. We assumed that the translocation of SITR1 is not restricted, which is a diffusion process. SIRT1 induces active p53 to return to its inactive form [16]. Activated p53 promotes Mdm2 synthesis, and Mdm2 inhibits p53 via the ubiquitin proteasome pathway, forming a negative feedback loop [12]. In addition, activated p53 promotes the transcription of some Bh3 proteins to open the mitochondrial apoptosis pathway [10]. Free Bax in the cytoplasm is transformed by Bh3 into a form inserted in the outer mitochondrial membrane (Baxm) [17]. In resting cells, Bh3 synthesizes a complex with Bcl-2, and its enzymatic activity is inhibited. Baxm can also bind to Bcl-2, thus releasing the inhibition of Bcl-2 on Bh3, forming a positive feedback loop [10]. We hypothesize that p53 deacetylated by SIRT1 in the cytoplasm can complex with Bcl-2, depending on the ability of SIRT1 to facilitate mitochondrial-dependent apoptosis [9]. See Appendix for dynamic equations.

Figure 1 Schematic diagram of the model. Pn and Pc represent the protein P in the nucleus and cytoplasm, respectively; the 'a' and 'p' at the end of the protein represent acetylation and phosphorylation, respectively; the 'm' at the end of the protein represents the protein inlaid on the outer mitochondrial membrane.

Apoptosis driven by different kinds of stress

Similar to the Ref. [18], this article considers three types of stress, namely constant stress, periodic stress, and decay stress. Constant stress may be more suitable for long-lasting stimuli that do not cause p53 oscillations, such as hypoxia [19]. Periodic stress may be more suitable for the type of stimulus that causes DNA double-strand breaks and further p53 oscillations. Since the oscillations of p53 are transmitted through the upstream ATM oscillations [20], this is equivalent to pressure oscillations. Decay stress is more suitable for the type of stimulus that acts on cells instantaneously, such as ultraviolet radiation [21]. This model regards Baxmtotal reaching a high steady state as a sign of cell apoptosis initiation. As shown in Figs. 2 3 4, p53c and p53na both increase to a relatively high level when apoptosis occurs, which is consistent with the experimental reports that p53 promotes apoptosis in a transcription-dependent and transcription-independent manner [22, 23].

Figure 2 Time courses of stress, p53c, p53na, and Baxmtotal. Here $[\mathrm{Stress}]' = 0$, and the initial stress=1 in (a), =2 in (b).

In the case of constant stress, high-intensity stress is conducive to rapid initiation of apoptosis. Comparing Fig. 2(a) and (b), the time when the apoptosis starts under the condition of stress=1 is significantly later than that under the condition of stress = 2. This is because high-intensity stress on the one hand can accelerate the accumulation of p53na and p53c, on the other hand, it can induce p53c and p53na to reach a higher steady state. In other words, increased cytotoxicity stress is always helpful to clean up the cells. And too low stress is not enough to cause Baxmtotal to reach high steady state and apoptosis.

Figure 3 Time courses of stress, p53c, p53na, and Baxmtotal. Here $[\mathrm{Stress}]' = Amplitude(2\pi/Period)\cos(2\pi t/Period)$, and the initial stress=0.5 in (a), (b), and (c), =1 in (d); $Amplitude$=1 in (a), (b), and (c), =2 in (d); $Period$=50 in (a) and (d), =100 in (b), =150 in (c).

In Fig. 3, we use a sine function to represent the periodic stress. In this case, there is an optimal time period that is most conducive to apoptosis. Taking Fig. 3(a) and (b) to compare, it can be seen that p53c and p53na gradually accumulate in the pulse, and low-frequency oscillation is dominant for apoptosis. However, this is not always the case. In the comparison of Fig. 3(b) and (c), the onset of apoptosis induced by lower frequency oscillations is later. This phenomenon also suggests that it is necessary to pay attention to the cycle of cytotoxic drugs to eliminate cancer cells. The rhythm of stress in Fig. 3(d) is the same as that of Fig. 3(a), but when the amplitude of stress doubles, the appearance of apoptosis is clearly advanced, which is similar to the case of constant stress.

Figure 4 Time courses of stress, p53c, p53na, and Baxmtotal. Here $[\text{Stress}]' = -k[\text{Stress}]$, and the initial stress=1 in (a) and (b), =2 in (c); k=0.002 in (a) and (c), =0.001 in (b).

Fig. 4 depicts the apoptotic situations under decreasing stress. In general, exponential decay is the most common way, and the speed of decay is negatively related to the half period of stress. The time series graphs of p53na and p53c under decreasing stress are like constant stress scenarios. The difference is that decreasing stress induces apoptosis depends on two factors, i.e. decay rete and initial conditions. The difference between Fig. 4(a) and (b) is that the latter has a lower decay rate of stress, which demonstrates that a small decay rate is beneficial to apoptosis. In addition, Fig. 4(a) and (c) illustrate that the greater the initial stress, the faster the time for apoptosis to occur at the same decay rate. In a nutshell, high-intensity stress in any type will be more prone to cause cell death.

The two sides of SIRT1

In this section, we tested the impact of different SIRT1 production rates on the onset of apoptosis. Regardless of the type of pressure, Fig. 5 exhibited that up-regulation or down-regulation of SIRT1 can delay the onset of apoptosis. This means that SIRT1 can not only act as a tumor promoter, but also as a tumor suppressor. Experimentally, it was initially reported that SIRT1 levels were up-regulated in some tumor cell lines, confirming that SIRT1 has a promoting effect on the formation of cancer and revealing the dark side of SIRT1 [24, 25]. However, subsequent experimental reports pointed out that SIRT1 also has a bright side. There are reports indicating that the levels of SIRT1 detected in breast and liver cancer are significantly reduced, providing evidence that SIRT1 has a tumor suppressor effect [26]. Therefore, our model may reconcile these seemingly contradictory conclusions about SIRT1 and cancer, that is, SIRT1 can promote apoptosis on the one hand, and inhibit apoptosis on the other. Perhaps there is a balanced level of SIRT1, where cells are most sensitive to apoptosis signals and have the best anti-cancer response.

Figure 5 Time courses of stress Baxmtotal. Here k_{ssirt} in the cases of the blue lines are less than the default value, and in the cases of the orange lines are greater than the default value. The stress situation of (a) is the same as Fig. 2(a); The stress situation of (b) is the same as Fig. 3(a); And the stress situation of (c) is the same as Fig. 4(a).

Codimension-two bifurcation analysis

To further illustrate the effect of both stress and SIRT1 production rate on system dynamics, bifurcation analysis is a technical way. In Fig. 6 we made the two-parameter bifurcation diagram of stress versus k_{ssirt} to characterize the dependence of the systems kinetics on the levels of SIRT1 and stress. These bifurcation curves divide this two-dimensional parameter plane into different parameter regions. According to the type of the surrounding bifurcation lines, in each parameter region, the system will have different dynamic features:

- R_1: typical monostability (one stable equilibrium point).
- $R_{1'}$: atypical monostability (one stable limit cycle).

•R_2: typical bistability (two stable equilibrium points).
•$R_{2'}$: atypical bistability (one stable equilibrium point and one stable limit cycle).
•R_3: excitebility (one stable equilibrium point coexists with two unstable equilibrium points).
•R_4: typical monostability (one stable equilibrium point).

Figure 6 Two-dimensional bifurcation diagram showing various types of bifurcation lines (Stress, k_{ssirt})-plane. The bifurcation lines divide the parameter domain into six subregions. Here SN stands for saddle node bifurcation, sup- or sub-HB stands for supercritical or subcritical Hopf bifurcation.

If the parameters are unvaried, apoptosis is bound to occur in R_3 and R_4 regions, is possible in R_2 and $R_{2'}$ regions, and is impossible in R_1 and $R_{1'}$ regions. Obviously, according to the shapes of the SN2 and sub-HB bifurcation curves, the optimal value range of k_{ssirt} for the occurrence of apoptosis is within interval $[10^{-3}, 10^{-2}]$.

Codimension-one bifurcation analysis

To be reasonable, the correctness of the two-dimensional bifurcation diagram should be verified, and the dynamics of Baxmtotal varying with the parameters should be explained. Therefore, we made a group of one-parameter bifurcation graphs in Fig. 7.

The scenarios of SIRT1 overexpression, moderate expression, and low expression are displayed in Fig. 7(a) from top to bottom. The bifurcation curve of the fixed point branch is folded into an "S" shape by two saddle node bifurcation points SN1 and SN2. The theoretical model indicates that if the content of SIRT1 is too high, the Baxmtotal switch in response to pressure can be toggled, that is to say, the Baxmtotal switch is opened when the pressure is applied, and is closed when the pressure is removed. Under such a mechanism, the lethality of the decay pressure on the cells may be totally destroyed, because the decay pressure will eventually become non-existent and Baxmtotal will eventually return to the basal level. In addition, the amplitudes of stable Baxmtotal oscillations born from supercritical Hopf bifurcation sup-HB are very small, which are far from the activated high concentration Baxmtotal level, so it may not have any effect on cell fate. The emergence of subcritical Hopf bifurcation causes the pressure threshold required for Baxmtotal activation to drop from SN2 to sub-HB. In these three bifurcation diagram examples, the moderately expressed SIRT1 has the smallest pressure threshold to initiate apoptosis. These are consistent with the aforementioned conclusions, namely too much or too little SIRT1 concentration will inhibit apoptosis and increase the risk of cancer.

We further made the one-dimensional bifurcation graphs of Baxmtotal as a function of k_{ssirt} under different stress situations in Fig. 7(b). When the stress is low, the main branch of the bifurcation curve is "Z"-shaped. Too high SIRT1 level will cause Baxmtotal to only have a low steady state, or oscillate near the low steady state, which reflects the role of SIRT1 as a carcinogen. On the contrary, under high stress, the main branch of the bifurcation curve is "S"-shaped and sufficient SIRT1 is beneficial for Baxmtotal to reach a high steady state, which reflects the tumor

suppressor effect of SIRT1. Interestingly, when the stress is moderate, the bifurcation curve has an "Ω" shape, which fully demonstrates the dual role of SIRT1 in p53-mediated apoptosis, i.e. SIRT1 concentration that is too high or too low can allow Baxmtotal to inhabit a low level similar to unstressed. It is worth noting that from the perspective of the time to initiate apoptosis, under high stress, it is not the higher SIRT1 level, the faster apoptosis initiation. Comparing Fig. 2(a) and Fig. 5(a), in the case of stress=1, $k_{\mathrm{ssirt}} = 10^{-2}$ initiates apoptosis faster than $k_{\mathrm{ssirt}} = 10^{-1}$. Thereby, it can be asserted that SIRT1 has two-sided effects on p53-induced apoptosis and even tumor formation in most cases.

Figure 7 One-dimensional bifurcation diagrams. SN, sup-HB, and sub-HB have the same meaning as Fig. 6. The stable and unstable steady states are indicated by red and black lines, respectively. Green lines are the maxima and minima of the stable limit cycles. The small picture is an enlargement of the oscillation interval.

Additionally, the dynamic distribution of the one-dimensional bifurcation graph set in Fig. 7 fits the two-dimensional bifurcation analysis. This also further confirms the correctness of our numerical bifurcation results.

Conclusion and discussion

Altogether, our numerical results indicate that STRT1 is an important factor for apoptosis regardless of the dynamic type of pressure the cell faces. Through bifurcation analysis, we characterized the dual role of SIRT1 on apoptosis (Baxmtotal switch) under cytotoxic pressure. Benign cells can always make proper fate management through internal protein network to avoid serious consequences, but transcription factor central network is disordered in some malignant cells, resulting in wrong cell outcomes [27]. In essence, SIRT1 finely regulates the balance between transcription-dependent and transcription-independent apoptosis of p53 [11]. As mentioned in Ref [7], this balance is essential for the cell fate determination mechanism. Our work explained that SIRT1 found in experiments sometimes suppresses cancer and sometimes promotes cancer from the perspective of theoretical model, and may be helpful for biomedical applications. In addition to the optimal level of SIRT1, this model also shows that there is an optimal period for cycle stress in initiating apoptosis. This is also something worth noting in practice.

Furthermore, miR-34 is the target of p53 positive regulation, which can hinder the translation of SIRT1 in some situations [28]. Based on the relationship between miR-34 and SIRT1 alone, miR-34 is a tumor-inhabiting factor when SIRT1 is abundantly expressed, or a tumor-promoting factor when SIRT1's expression is lacking. However, as far as we know, there is no report showing that miR-34 promotes tumor formation. As analyzed by our previous theoretical model, the tumor suppressor effect of miR-34 may be achieved also by inhibiting the E3 ubiquitin ligase function of Mdm2 [29]. Moreover, the BCL-2 family can also participate in autophagy [30]; The dynamic mode of the p53 module is also in charge of cell fate, and the theoretical model of p53 pulse or multi-stable steady state regulating cell fate refers to Refs.[31, 32]. Investigating the dynamics of p53 motifs is also an interesting study, and there have been some related researches [33, 34]. In short, biological theoretical models can reproduce the existing experimental phenomena, and can also explore

the field that experiments have not yet entered [35]. This is a fascinating part of systems biology.

Appendix: Dynamic equations

In the p53 module, enzymatic reactions follow the Michaelis-Menten kinetics [31], such as stress promotes p53 activation and Mdm2 degradation, Mdm2 promotes p53 degradation, and SIRT1 promotes p53 inactivation. Mdm2 phosphorylation and dephosphorylation are assumed to occur only in the cytoplasm [31], where enzymes (such as Akt) are not considered. p53 accelerates the production of target proteins in accordance with Hill dynamics [31]. Unlike the p53 module, in the Bcl-2 protein family module, Bh3 promotes the transformation of Bax to Baxm as a linear function [10]. The model did not include the form of the Bcl-2 family in the nucleus. For proteins that can be transported across membranes, entering the nucleus is a diffusion process [14], that is, the transport rate is related to the concentration difference and permeability. Moreover, in order to reproduce the bistable state of Baxmtotal, the total amount of Bax and Bcl-2 is assumed to be unchanged, and after binding to Bcl-2, the conversion of Baxm to free Bax, the degradation of Bh3 are not affected [10]. For simplicity, it is assumed that the biochemical reactions of degradation and activation of p53c after it form a complex with Bcl-2 do not occur. The equations are as follows:

$$\begin{aligned}\frac{\mathrm{d}[\mathrm{p53na}]}{\mathrm{d}t} &= (k_{\mathrm{acp530}} + k_{\mathrm{acp531}}\frac{[\mathrm{Stress}]}{[\mathrm{Stress}]+j_{\mathrm{stress}}})[\mathrm{p53n}] - k_{\mathrm{dep53}}\frac{[\mathrm{SIRT1n}]}{[\mathrm{SIRT1n}]+j_{\mathrm{sirt1}}}[\mathrm{p53na}] \\ &\quad -k_{\mathrm{dp53s}}[\mathrm{Mdm2np}]\frac{[\mathrm{p53na}]}{[\mathrm{p53na}]+j_{1\mathrm{p53}}} + V_{\mathrm{r}}k_{\mathrm{i}}[\mathrm{p53ca}],\end{aligned} \tag{1}$$

$$\begin{aligned}\frac{\mathrm{d}[\mathrm{p53n}]}{\mathrm{d}t} &= -(k_{\mathrm{acp530}} + k_{\mathrm{acp531}}\frac{[\mathrm{Stress}]}{[\mathrm{Stress}]+j_{\mathrm{stress}}})[\mathrm{p53n}] + k_{\mathrm{dep53}}\frac{[\mathrm{SIRT1n}]}{[\mathrm{SIRT1n}]+j_{\mathrm{sirt1}}}[\mathrm{p53na}] \\ &\quad -k_{\mathrm{dp53}}[\mathrm{Mdm2np}]\frac{[\mathrm{p53n}]}{[\mathrm{p53n}]+j_{1\mathrm{p53}}} - k_{\mathrm{dp530}}[\mathrm{p53n}] + V_{\mathrm{r}}k_{\mathrm{i}}([\mathrm{p53c}] - [\mathrm{p53n}]),\end{aligned} \tag{2}$$

$$\begin{aligned}\frac{\mathrm{d}[\mathrm{p53c}]}{\mathrm{d}t} &= k_{\mathrm{sp53}} - k_{\mathrm{acp530}}[\mathrm{p53c}] + k_{\mathrm{dep53}}\frac{[\mathrm{SIRT1c}]}{[\mathrm{SIRT1c}]+j_{\mathrm{sirt1}}}[\mathrm{p53ca}] - k_{\mathrm{dp53}}([\mathrm{Mdm2cp}] \\ &\quad +[\mathrm{Mdm2c}])\frac{[\mathrm{p53c}]}{[\mathrm{p53c}]+j_{1\mathrm{p53}}} - k_{\mathrm{dp530}}[\mathrm{p53c}] - k_{\mathrm{asp2}}[\mathrm{p53c}][\mathrm{Bcl}-2] \\ &\quad +k_{\mathrm{dsp2}}[\mathrm{p53c}\bullet\mathrm{Bcl}-2] - k_{\mathrm{i}}([\mathrm{p53c}] - [\mathrm{p53n}]),\end{aligned} \tag{3}$$

$$\begin{aligned}\frac{\mathrm{d}[\mathrm{p53ca}]}{\mathrm{d}t} &= k_{\mathrm{acp530}}[\mathrm{p53c}] - k_{\mathrm{dep53}}\frac{[\mathrm{SIRT1c}]}{[\mathrm{SIRT1c}]+j_{\mathrm{sirt1}}}[\mathrm{p53ca}] - k_{\mathrm{dp53s}}([\mathrm{Mdm2cp}] \\ &\quad +[\mathrm{Mdm2c}])\frac{[\mathrm{p53ca}]}{[\mathrm{p53ca}]+j_{1\mathrm{p53}}} - k_{\mathrm{i}}[\mathrm{p53ca}],\end{aligned} \tag{4}$$

$$\begin{aligned}\frac{\mathrm{d}[\mathrm{Mdm2c}]}{\mathrm{d}t} &= k_{\mathrm{smdm20}} + k_{\mathrm{smdm2}}\frac{[\mathrm{p53na}]^4}{[\mathrm{p53na}]^4+j_{\mathrm{smdm2}}^4} - k_{\mathrm{dmdm20}}[\mathrm{Mdm2c}] \\ &\quad +k_{1\mathrm{mdm2s}}\frac{[\mathrm{Mdm2cp}]}{[\mathrm{Mdm2cp}]+j_{1\mathrm{mdm2s}}} - k_{\mathrm{mdm2s}}\frac{[\mathrm{Mdm2c}]}{[\mathrm{Mdm2c}]+j_{\mathrm{mdm2s}}},\end{aligned} \tag{5}$$

$$\begin{aligned}\frac{\mathrm{d}[\mathrm{Mdm2cp}]}{\mathrm{d}t} &= -k_{1\mathrm{mdm2s}}\frac{[\mathrm{Mdm2cp}]}{[\mathrm{Mdm2cp}]+j_{1\mathrm{mdm2s}}} + k_{\mathrm{mdm2s}}\frac{[\mathrm{Mdm2c}]}{[\mathrm{Mdm2c}]+j_{\mathrm{mdm2s}}} \\ &\quad -k_{\mathrm{dmdm20}}[\mathrm{Mdm2cp}] - k_{\mathrm{i}}([\mathrm{Mdm2cp}] - [\mathrm{Mdm2np}]),\end{aligned} \tag{6}$$

$$\frac{\mathrm{d}[\mathrm{Mdm2np}]}{\mathrm{d}t} = -(k_{\mathrm{dmdm20}} + k_{\mathrm{dmdm21}}\frac{[\mathrm{Stress}]}{[\mathrm{Stress}]+j_{\mathrm{stress}}})[\mathrm{Mdm2np}] + V_{\mathrm{r}}k_{\mathrm{i}}([\mathrm{Mdm2cp}]-[\mathrm{Mdm2np}]), \tag{7}$$

$$\frac{\mathrm{d}[\mathrm{SIRT1c}]}{\mathrm{d}t} = k_{\mathrm{ssirt}} - k_{\mathrm{dsirt}}[\mathrm{SIRT1c}] - k_{\mathrm{i}}([\mathrm{SIRT1c}] - [\mathrm{SIRT1n}]), \tag{8}$$

$$\frac{\mathrm{d}[\mathrm{SIRT1n}]}{\mathrm{d}t} = -k_{\mathrm{dsirt}}[\mathrm{SIRT1n}] + V_{\mathrm{r}}k_{\mathrm{i}}([\mathrm{SIRT1c}] - [\mathrm{SIRT1n}]), \tag{9}$$

$$[\mathrm{Bax}] = [\mathrm{Baxtotal}] - [\mathrm{Baxmtotal}], \tag{10}$$

$$[\mathrm{Baxm} \bullet \mathrm{Bcl}-2] = [\mathrm{Baxmtotal}] - [\mathrm{Baxm}], \tag{11}$$

$$[\mathrm{Bh3} \bullet \mathrm{Bcl}-2] = [\mathrm{Bh3total}] - [\mathrm{Bh3}], \tag{12}$$

$$[\mathrm{Bcl}-2] = [\mathrm{Bcl}-2\mathrm{total}] - [\mathrm{Bh3} \bullet \mathrm{Bcl}-2] - [\mathrm{Baxm} \bullet \mathrm{Bcl}-2] - [\mathrm{p53c} \bullet \mathrm{Bcl}-2], \tag{13}$$

$$\frac{\mathrm{d}[\mathrm{p53c} \bullet \mathrm{Bcl}-2]}{\mathrm{d}t} = k_{\mathrm{asp2}}[\mathrm{p53c}][\mathrm{Bcl}-2] - k_{\mathrm{dsp2}}[\mathrm{p53c} \bullet \mathrm{Bcl}-2], \tag{14}$$

$$\frac{\mathrm{d}[\mathrm{Baxm}]}{\mathrm{d}t} = (k_{\mathrm{f1}} + k_{\mathrm{f2}}[\mathrm{Bh3}])[\mathrm{Bax}] - k_{\mathrm{asx2}}[\mathrm{Baxm}][\mathrm{Bcl}-2] + k_{\mathrm{dsx2}}[\mathrm{Baxm} \bullet \mathrm{Bcl}-2] - k_{\mathrm{b}}[\mathrm{Baxm}], \tag{15}$$

$$\frac{\mathrm{d}[\mathrm{Bh3}]}{\mathrm{d}t} = k_{\mathrm{sbh30}} + k_{\mathrm{sbh31}}\frac{[\mathrm{p53na}]^4}{[\mathrm{p53na}]^4 + j_{\mathrm{sbh3}}^4} - k_{\mathrm{as32}}[\mathrm{Bh3}][\mathrm{Bcl}-2] + k_{\mathrm{ds32}}[\mathrm{Bh3} \bullet \mathrm{Bcl}-2] - k_{\mathrm{dbh3}}[\mathrm{Bh3}], \tag{16}$$

$$\frac{\mathrm{d}[\mathrm{Baxmtoal}]}{\mathrm{d}t} = (k_{\mathrm{f1}} + k_{\mathrm{f2}}[\mathrm{Bh3}])[\mathrm{Bax}] - k_{\mathrm{b}}[\mathrm{Baxmtotal}]. \tag{17}$$

$$\frac{\mathrm{d}[\mathrm{Bh3toal}]}{\mathrm{d}t} = k_{\mathrm{sbh30}} + k_{\mathrm{sbh31}}\frac{[\mathrm{p53na}]^4}{[\mathrm{p53na}]^4 + j_{\mathrm{sbh3}}^4} - k_{\mathrm{dbh3}}[\mathrm{Bh3total}], \tag{18}$$

Here [] means the concentration, and A•B represents the complex of proteins A and B. Since we focus on qualitative rather than quantitative issues, the units of time and concentration have not been introduced. The parameters are in the Table 1 below.

Table 1. Simulation parameters.

Parameter	Description	Value	Reference
k_{acp530}	p53 basal activation rate	0.02	-
k_{acp531}	Stress-induced the maximum p53 activation rate	0.2	[31]
k_{dmdm20}	Mdm2 basal degradation rate	0.003	[31]
k_{dmdm21}	Stress-induced the maximum Mdm2 degradation rate	0.05	[31]
j_{stress}	Michaelis constant of stress as a kinase	1	[31]
k_{dep53}	SIRT1-induced the maximum p53 deactivation rate	0.4	-
j_{sirt1}	Michaelis constant of SIRT1 as a kinase	0.1	-
k_{dp53s}	Mdm2-induced the maximum active p53 degradation rate	0.01	[31]
j_{1p53}	Michaelis constant of Mdm2 as a kinase	0.1	[31]
k_{dp53}	Mdm2-induced the maximum inactive p53 degradation rate	0.7	[31]
k_{dp530}	p53 basal degradation rate	0.05	[31]
k_{sp53}	p53 basal generation rate	0.2	[31]
k_{smdm20}	Mdm2 basal generation rate	0.002	[31]
k_{smdm2}	p53-dependent Mdm2 generation rate	0.024	[31]
j_{smdm2}	Michaelis constant of p53-dependent Mdm2 production	1	[31]
k_{1mdm2s}	Dephosphorylation rate of cytoplasmic Mdm2	0.3	[31]
j_{1mdm2s}	Michaelis constant of Mdm2 dephosphorylation	0.1	[31]
k_{mdm2s}	Phosphorylation rate of cytoplasmic Mdm2	8	[31]
j_{mdm2s}	Michaelis constant of Mdm2 phosphorylation	0.3	[31]
k_{ssirt}	SIRT1 basal generation rate	0.01	-
k_{dsirt}	SIRT1 basal degradation rate	0.1	-
V_{r}	Cytoplasm to nucleus volume ratio	10	[14]
k_{i}	Protein penetration rate of the nuclear membrane	0.06	-
k_{asp2}	Combination rate of p53 and Bcl-2	0.8	-
k_{dsp2}	Dissociation rate of p53 and Bcl-2 complex	0.1	-
k_{f1}	Basal rate of Bax to Baxm conversion	1	[10]
k_{f2}	Bh3-induced rate of Bax to Baxm conversion	3	[10]
k_{asx2}	Combination rate of Baxm and Bcl-2	90	[10]
k_{dsx2}	Dissociation rate of Baxm and Bcl-2 complex	0.05	[10]
k_{b}	Basal rate of Baxm to Bax conversion	2	[10]
k_{sbh30}	Bh3 basal generation rate	0.1	-
k_{sbh31}	p53-dependent Bh3 generation rate	0.306	-
j_{sbh3}	Michaelis constant of p53-dependent Bh3 production	0.01	-
k_{as32}	Combination rate of Bh3 and Bcl-2	90	[10]
k_{ds32}	Dissociation rate of Bh3 and Bcl-2 complex	0.01	[10]
k_{dbh3}	Bh3 basal degradation rate	0.01	[10]
$[\mathrm{Baxtotal}]$	Total level of Bax	100	[10]
$[\mathrm{Bcl-2total}]$	Total level of Bcl-2	80	[10]

The initial conditions in the Table 2 select the steady-state set of each protein concentration corresponding to the low steady state of Baxmtotal when there is no stress.

Table 2. Initial condition.

Protein	Initial	Protein	Initial	Protein	Initial	Protein	Initial
$[\mathrm{p53na}]$	0.01	$[\mathrm{p53n}]$	0.01	$[\mathrm{p53ca}]$	0.01	$[\mathrm{p53c}]$	0.08
$[\mathrm{Mdm2c}]$	0.01	$[\mathrm{Mdm2cp}]$	0.6	$[\mathrm{Mdm2np}]$	0.59	$[\mathrm{SIRT1c}]$	0.09
$[\mathrm{SIRT1n}]$	0.08	$[\mathrm{p53 \bullet Bcl-2}]$	4.2	$[\mathrm{Baxm}]$	0.12	$[\mathrm{Bh3}]$	0.01
$[\mathrm{Baxmtotal}]$	34.06	$[\mathrm{Bh3total}]$	35.44				

All numerical simulations and bifurcation analysis are completed with free software:
XPPAUT (http://www.math.pitt.edu/ bard/xpp/xpp.html),
OSCILL8 (http://oscill8.sourceforge.net/).

Funding

This work was supported by National Natural Science Foundation of China (Grants No. 11762011).

Abbreviations

SIRT1: Sirtuin1.
BCL-2: B-cell lymphoma-2.
Bax: BCL2-Associated X protein.
Bcl-2: B-cell lymphoma-2 protein.
Bh3: Bcl-2 homology domain only proteins.
Puma: P53 up-regulated modulator of apoptosis.
p53: p53 protein.
Mdm2: Murine double minute 2 protein.
DNA: DeoxyriboNucleic Acid.
p53n: p53 in the nucleus.
p53c: p53 in the cytoplasm.
Mdm2c: p53 in the cytoplasm.
p53na: Activated p53 in the nucleus.
p53ca: Activated p53 in the cytoplasm.
Mdm2np: Phosphorylated Mdm2 in the cytoplasm.
Mdm2cp: Phosphorylated Mdm2 in the cytoplasm.
Baxm: Bax in the outer mitochondrial membrane.

Baxmtotal: Total level of Baxm.
Bcl-2total: Total level of Bcl-2.
Bh3total: Total level of Bh3.
SIRT1n: SIRT1 in the nucleus.
SIRT1c: SIRT1 in the cytoplasm.
Baxm• Bcl-2: Baxm and Bcl-2 complex.
Bh3• Bcl-2: Bh3 and Bcl-2 complex.
p53• Bcl-2: p53c and Bcl-2 complex.
SN: Saddle node bifurcation.
HB: Hopf bifurcation.
sup-HB: supercritical Hopf bifurcation.
sub-HB: subcritical Hopf bifurcation.

Availability of data and materials

All data used and analyzed during the current study available from the corresponding author on reasonable request.

Ethics approval and consent to participate

Not applicable

Competing interests

The authors declare that they have no competing interests.

Consent for publication

Not applicable

Authors' contributions

NL and HLY constructed the theoretical model, performed the numerical simulations, analyzed the data. LGY provided the ideas. All authors participated in writing the manuscript.

References

1. Johnstone RW, Ruefli AA, Lowe SW. Apoptosis: a link between cancer genetics and chemotherapy[J]. Cell. 2002;108(2):153-164.
2. Schleich K, Lavrik IN. Mathematical modeling of apoptosis[J]. Cell Commun Signal. 2013;11(1):44.
3. Sun T, Lin X, Wei Y, et al. Evaluating bistability of Bax activation switch[J]. FEBS Lett. 2010;584(5):954-960.
4. Youle RJ, Strasser A. The BCL-2 protein family: opposing activities that mediate cell death[J]. Nat Rev Mol Cell Biol. 2008;9(1):47-59.
5. Tang Y, Luo J, Zhang W, et al. Tip60-dependent acetylation of p53 modulates the decision between cell-cycle arrest and apoptosis[J]. Mol Cell. 2007;24(6):827-839.
6. Mihara M, Erster S, Zaika A, et al. P53 has a direct apoptogenic role at the mitochondria[J]. Mol Cell. 2003;11(3):577-590.
7. Pu T, Zhang XP, Liu F, et al. Coordination of the nuclear and cytoplasmic activities of p53 in response to DNA damage[J]. Biophys J. 2010;99(6):1696-1705.
8. Tian XJ, Liu F, Zhang XP, et al. A two-step mechanism for cell fate decision by coordination of nuclear and mitochondrial p53 activities[J]. PLoS One. 2012;7(6):e38164.
9. Han M, Song E, Guo Y, et al. SIRT1 regulates apoptosis and nanog expression in mouse embryonic stem cells by controlling p53 subcellular localization[J]. Cell Stem Cell. 2008;2(3):241-251.
10. Zhang T, Brazhnik P, Tyson JJ. Computational analysis of dynamical responses to the intrinsic pathway of programmed cell death[J]. Biophys J. 2009;97(2):415-434.
11. Yi J, Luo J. SIRT1 and p53, effect on cancer, senescence and beyond[J]. Biochim Biophys Acta. 2010;1804(8):1684-1689.
12. Lev BR, Maya R, Segel L A, et al. Generation of oscillations by the p53-Mdm2 feedback loop: A theoretical and experimental study[J]. Proc Natl Acad Sci USA. 2000;97(21):11250-11255.
13. Zhang TL, Brazhnik P, Tyson JJ. Exploring mechanisms of the DNA-damage response: p53 pulses and their possible relevance to apoptosis[J]. Cell Cycle. 2007;6(1):85-94.
14. Eliaš J, Dimitrio L, Clairambault J, et al. The dynamics of p53 in single cells: physiologically based ODE and reaction-diffusion PDE models[J]. Phys Biol. 2014;11(4):045001.
15. Mayo LD, Donner DB. A phosphatidylinositol 3-kinase/Akt pathway promotes translocation of Mdm2 from the cytoplasm to the nucleus[J]. Proc Natl Acad Sci USA. 2001;98(20):11598-11603.
16. Vaziri H, Dessain SK, Eaton EN, et al. Hsir2 (sirt1) functions as an nad-dependent p53 deacetylase[J]. Cell. 2001;107(2):149-159.
17. Marani M, Tenev T, Hancock D, et al. Identification of novel isoforms of the BH3 domain protein Bim which directly activate Bax to trigger apoptosis[J]. Mol Cell Biol. 2002;22(11):3577-3589.
18. Jangid A, Malik MZ, Ramaswamy R, et al. Transition and identification of pathological states in p53 dynamics for therapeutic intervention[J]. Sci Rep. 2021;11(1):2349.
19. Zhou CH, Zhang XP, Liu F, et al. Modeling the interplay between the HIF-1 and p53 pathways in hypoxia[J]. Sci Rep. 2015;5(6):13834.
20. Batchelor E, Mock CS, Bhan I, et al. Recurrent initiation: a mechanism for triggering p53 pulses in response to DNA Damage[J]. Mol Cell. 2008;30(3):277-289.
21. Li H, Zhang XP, Liu F. Coordination between p21 and DDB2 in the cellular response to UV radiation[J]. PLoS One. 2013;8(11):e80111.
22. Min S, Kim K, Kim SG, et al. Chromatin-remodeling factor, RSF1, controls p53-mediated transcription in apoptosis upon DNA strand breaks[J]. Cell Death Dis. 2018;9:1079.

23. Bonini P, Cicconi S, Cardinale A, et al. Oxidative stress induces p53-mediated apoptosis in glia: p53 transcription-independent way to die[J]. J Neurosci Res. 2004;75(1):83-95.
24. Huffman DM, Grizzle WE, Bamman MW, et al. SIRT1 is significantly elevated in mouse and human prostate cancer[J]. Cancer Res. 2007;67(14):6612-6618.
25. Stünkel W, Peh BK, Tan YC, et al. Function of the SIRT1 protein deacetylase in cancer[J]. Biotechnol J. 2010;2(11):1360-1368.
26. Wang RH, Sengupta K, Li C, et al. Impaired DNA damage response, genome instability, and tumorigenesis in SIRT1 mutant mice[J]. Cancer Cell. 2008;14(4):312-323.
27. Albrecht M, Lucarelli P, Kulms D, et al. Computational models of melanoma[J]. Theor Biol Med Model. 2020;17:8.
28. Hermeking H. MicroRNAs in the p53 network: micromanagement of tumour suppression[J]. Nat Rev Cancer. 2012;12(9):613-626.
29. Liu N, Yang HL, Yang LG. Exploring the influence of microRNA miR-34 on p53 dynamics: a numerical study[J]. Commun Theor Phys. 2021;73(3):035601.
30. Yang BJ, Liu QS, Bi YH. Autophagy and apoptosis are regulated by stress on Bcl2 by AMBRA1 in the endoplasmic reticulum and mitochondria[J]. Theor Biol Med Model. 2019;16:18.
31. Zhang XP, Liu F, Wang W. Two-phase dynamics of p53 in the DNA damage response[J]. Proc Natl Acad Sci USA. 2011;108(22):8990-8995.
32. Zhang XP, Liu F, Wang W. Regulation of the DNA damage response by p53 cofactors[J]. Biophys J. 2012;102(10):2251-2260.
33. Liu N, Yang HL, Li SS, et al. Oscillation and bistable switching dynamical behavior of p53 regulated by PTEN upon DNA damage[J]. Acta Mech Sin. 2021;Online First(https://doi.org/10.1007/s10409-020-01041-3).
34. Bi YH, Liu QS, Wang LX, et al. Bifurcation and potential landscape of p53 dynamics depending on PDCD5 level and ATM degradation rate[J]. Int J Bifurcat Chaos. 2020;30(09):2050134.
35. Kitano H. Systems biology: a brief overview[J]. Science. 2002;295(5560):1662-1664.

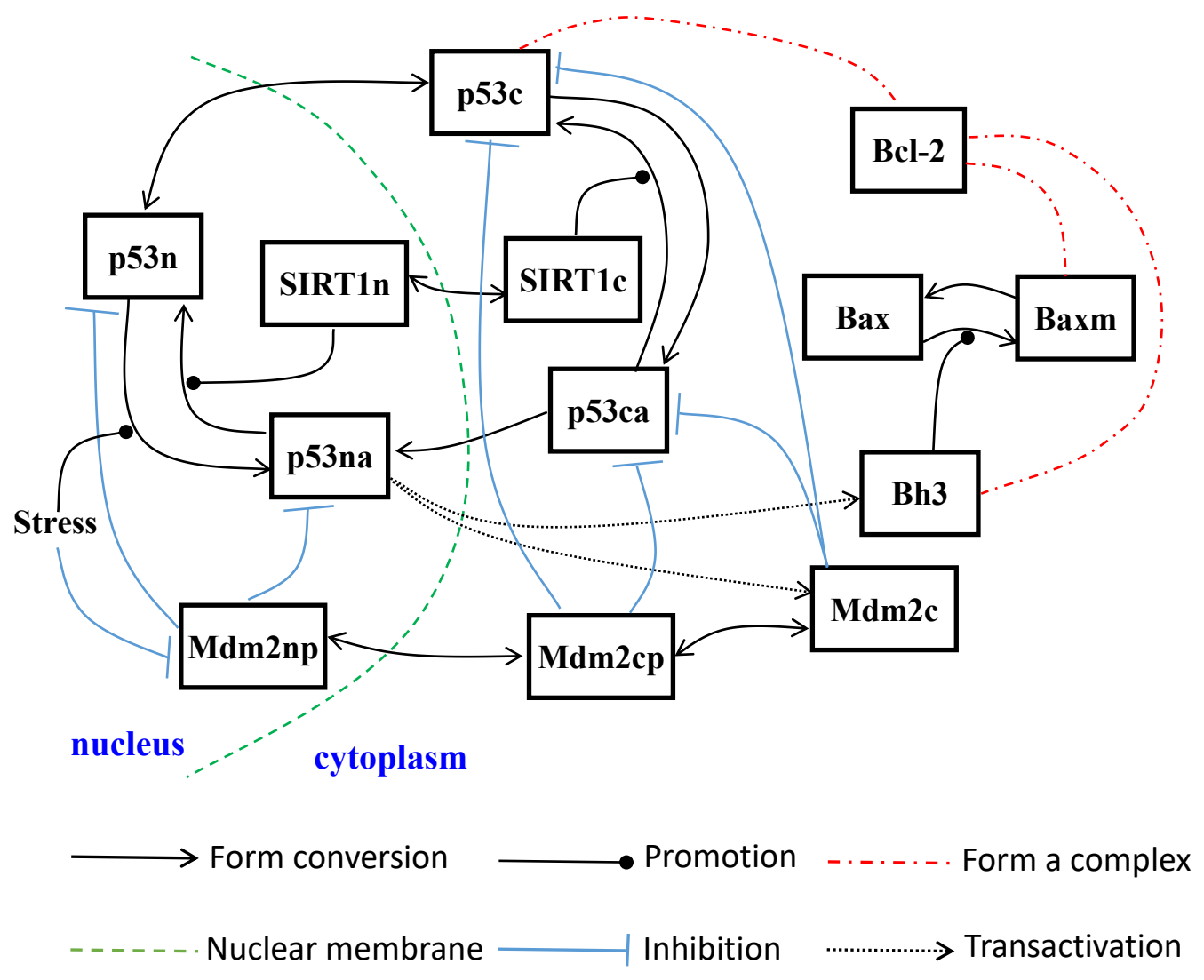
p53c
Bcl-2
p53n
SIRT1n
SIRT1c
Bax
Baxm
p53ca
p53na
Bh3
Stress
Mdm2c
Mdm2np
Mdm2cp
nucleus
cytoplasm
Form conversion
Promotion
Form a complex
Nuclear membrane
Inhibition
Transactivation

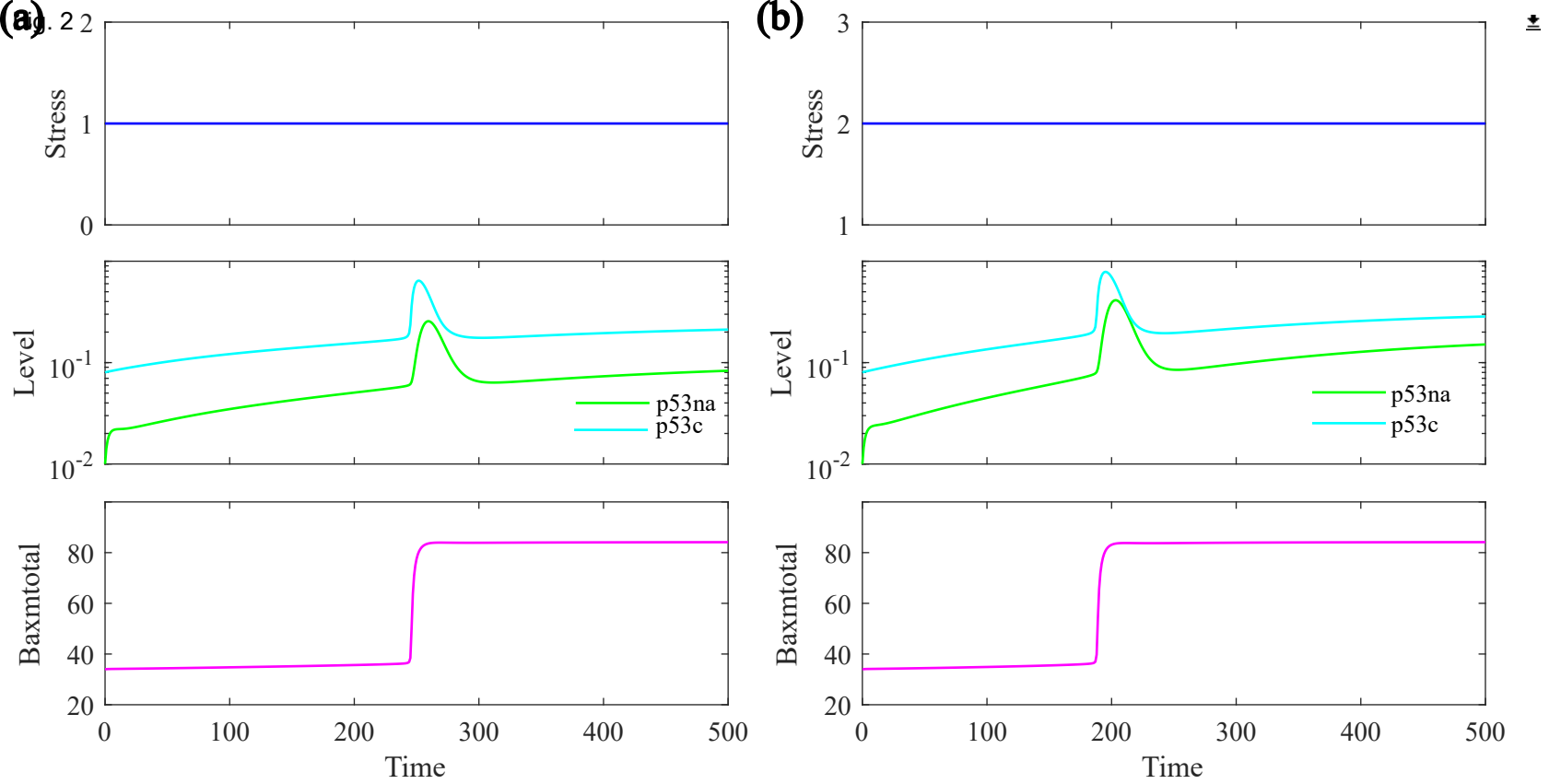
(a)
(b)
Stress
Level
Baxmtotal
Time
p53na
p53c

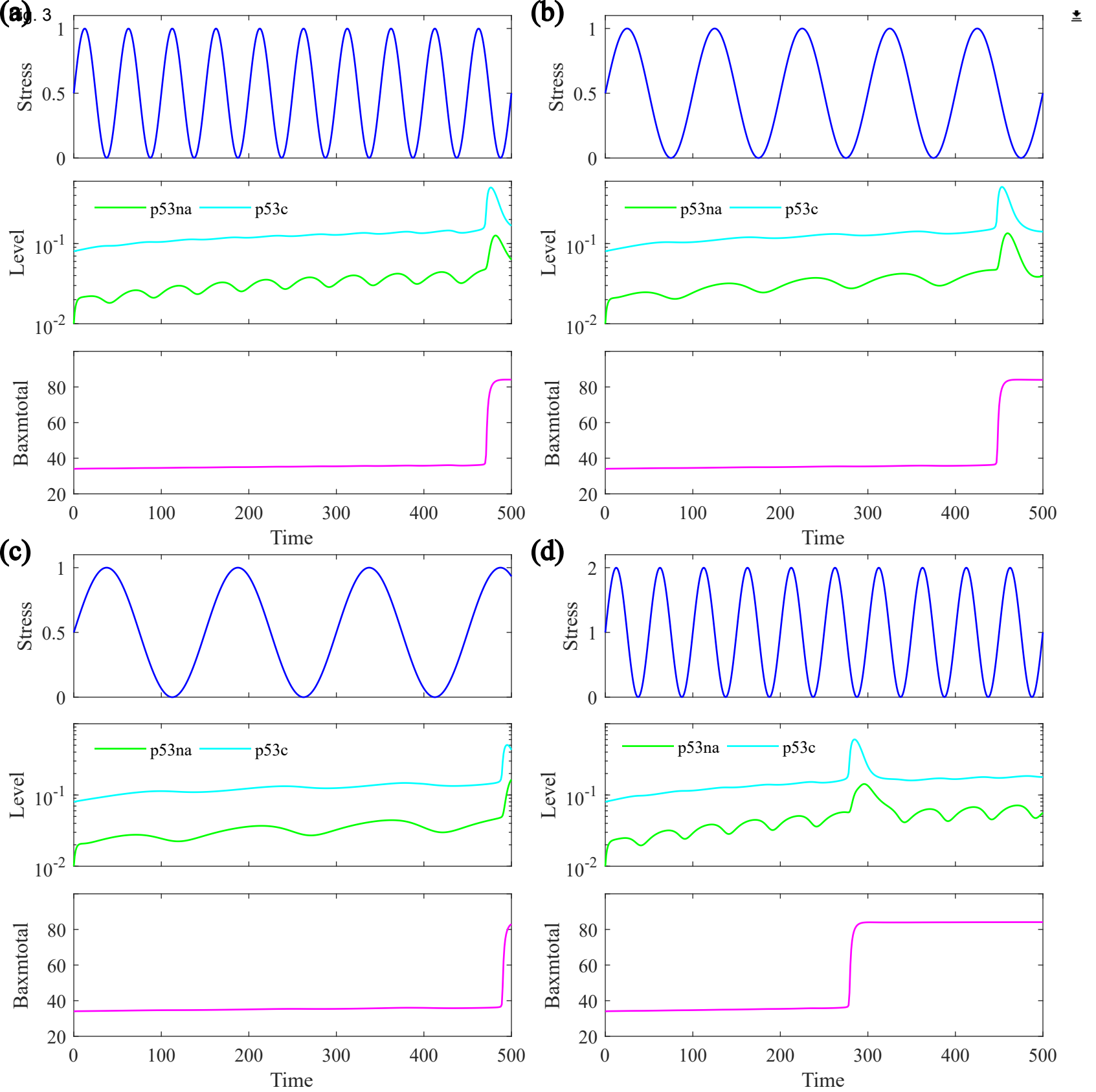
(a)
(b)
(c)
(d)
Stress
Level
Baxmtotal
p53na
p53c
Time

Fig. 4

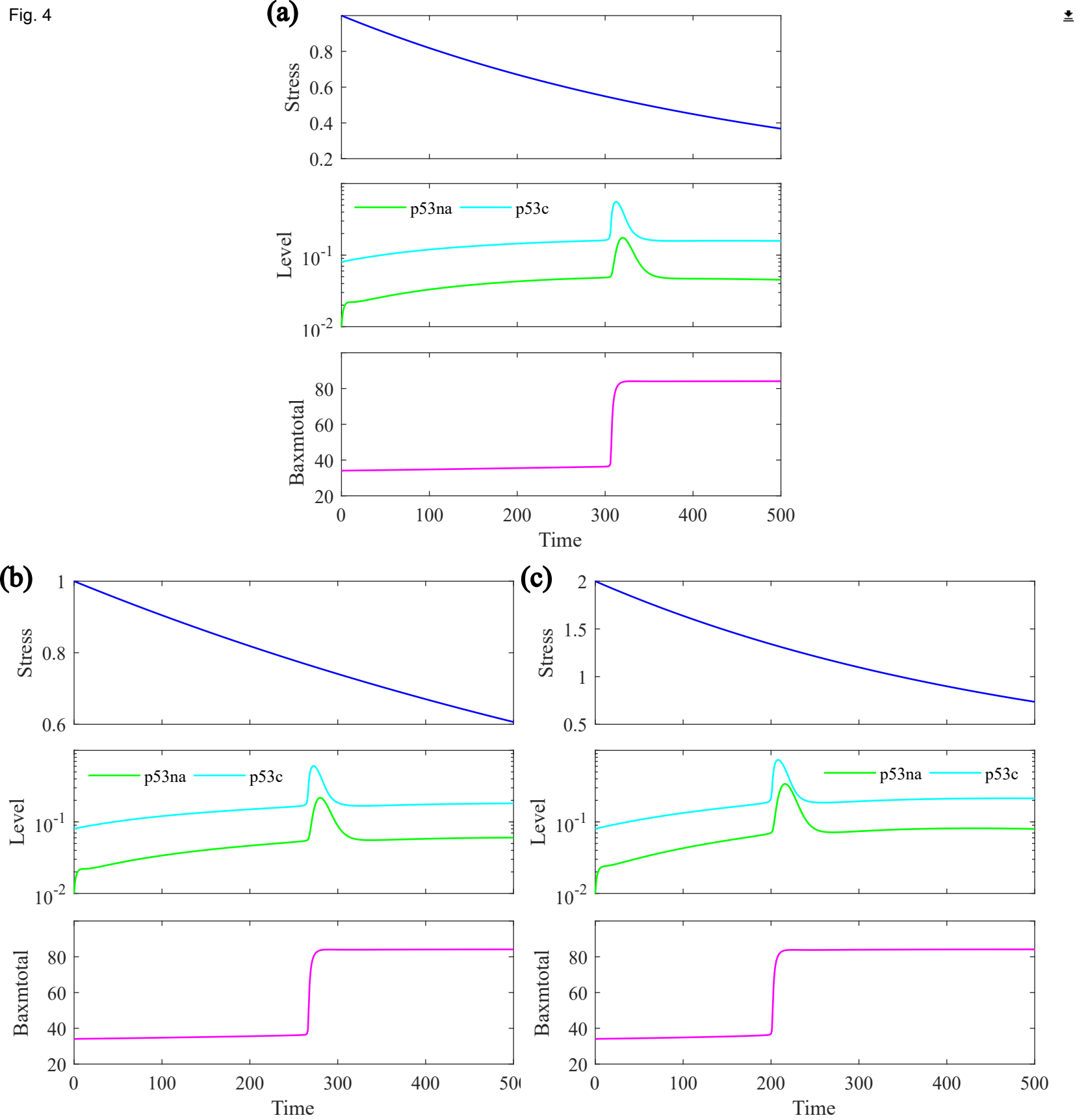
(a)
Stress
0.8
0.6
0.4
0.2
Level
p53na
p53c
10^{-1}
10^{-2}
Baxmtotal
80
60
40
20
0
100
200
300
400
500
Time
(b)
Stress
1
0.8
0.6
Level
p53na
p53c
10^{-1}
10^{-2}
Baxmtotal
80
60
40
20
0
100
200
300
400
Time
(c)
Stress
2
1.5
1
0.5
Level
p53na
p53c
10^{-1}
10^{-2}
Baxmtotal
80
60
40
20
0
100
200
300
400
500
Time

Fig. 5

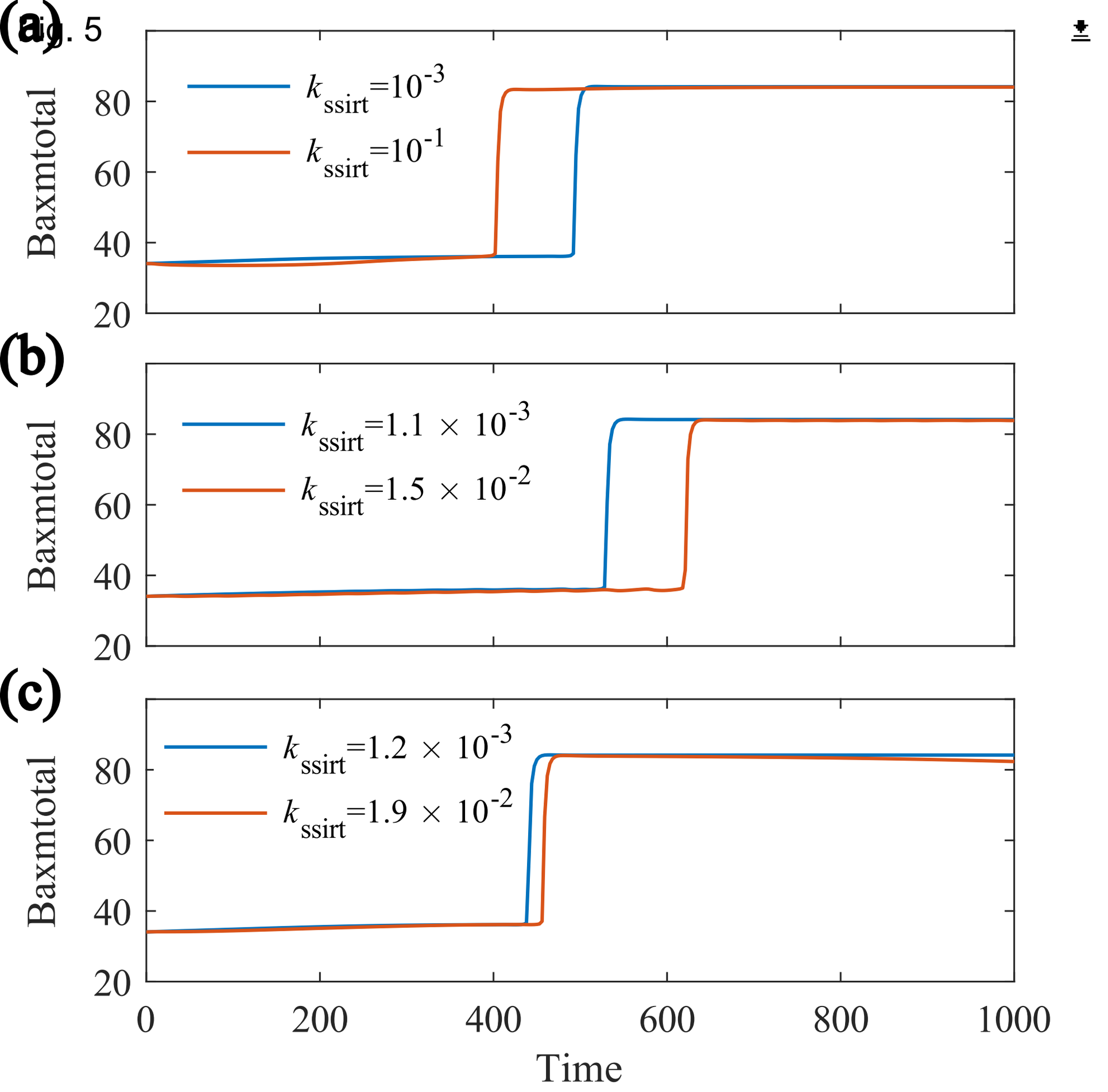
(a)
Baxmtotal
80
60
40
20
$k_{ssirt}=10^{-3}$
$k_{ssirt}=10^{-1}$
(b)
Baxmtotal
80
60
40
20
$k_{ssirt}=1.1 \times 10^{-3}$
$k_{ssirt}=1.5 \times 10^{-2}$
(c)
Baxmtotal
80
60
40
20
$k_{ssirt}=1.2 \times 10^{-3}$
$k_{ssirt}=1.9 \times 10^{-2}$
0
200
400
600
800
1000
Time

Fig. 6

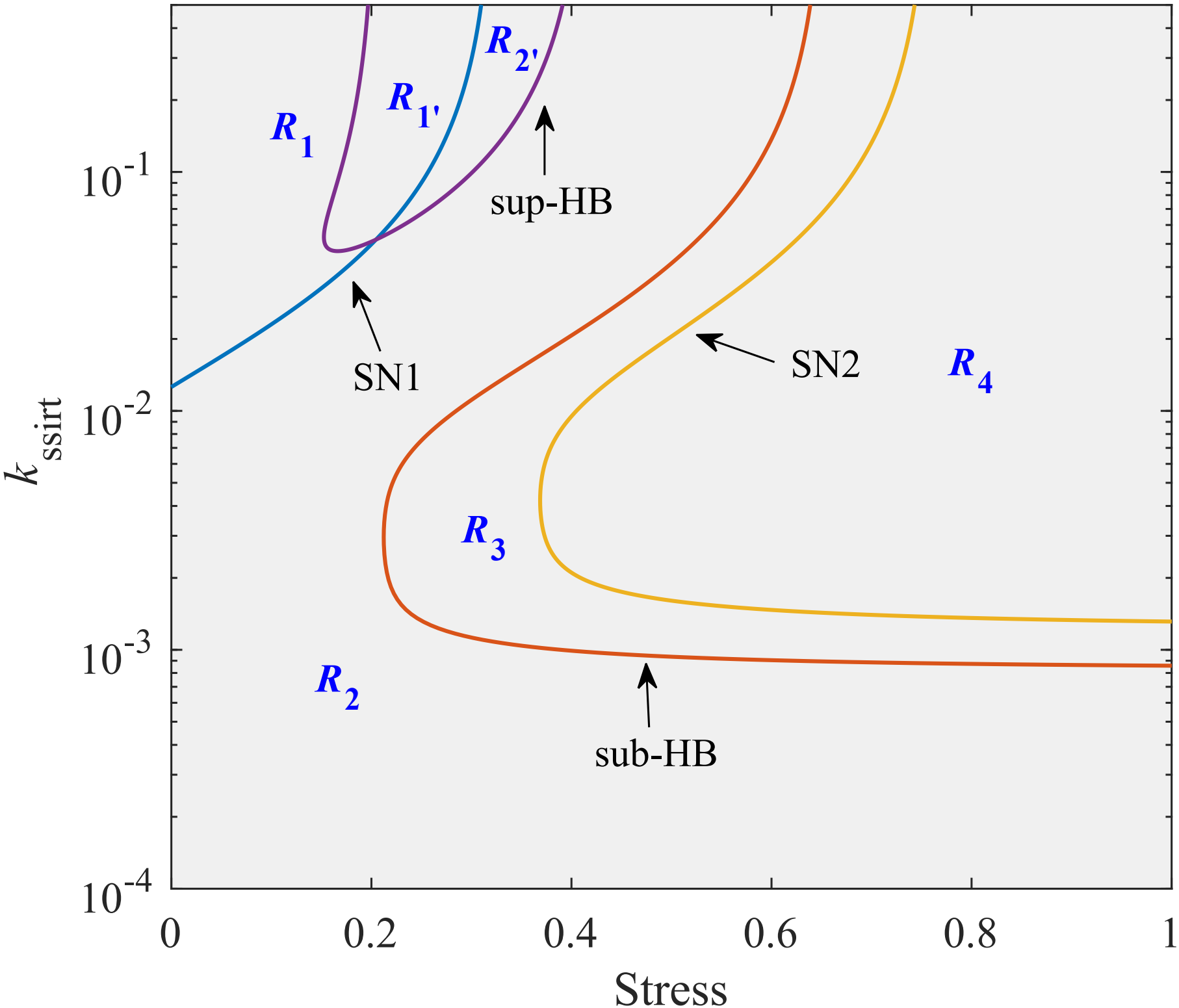
R_1
$R_{1'}$
$R_{2'}$
sup-HB
SN1
SN2
R_4
R_3
R_2
sub-HB
10^{-1}
10^{-2}
10^{-3}
10^{-4}
k_{ssirt}
0
0.2
0.4
0.6
0.8
1
Stress

Fig. 7

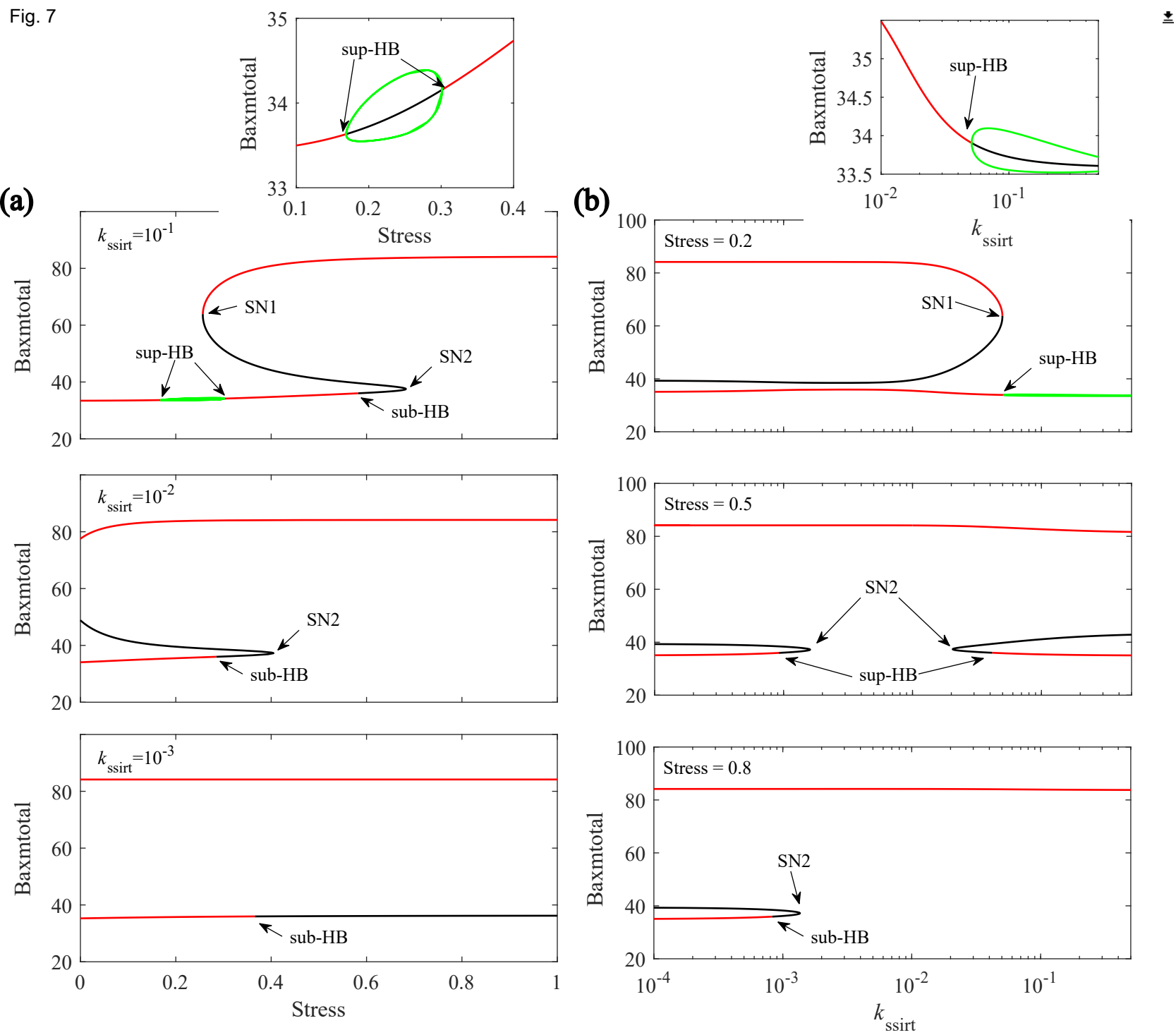
(a)
(b)
Baxmtotal
Stress
k_{ssirt}
k_{ssirt}=10^-1
k_{ssirt}=10^-2
k_{ssirt}=10^-3
SN1
SN2
sup-HB
sub-HB
Stress = 0.2
Stress = 0.5
Stress = 0.8

Figures

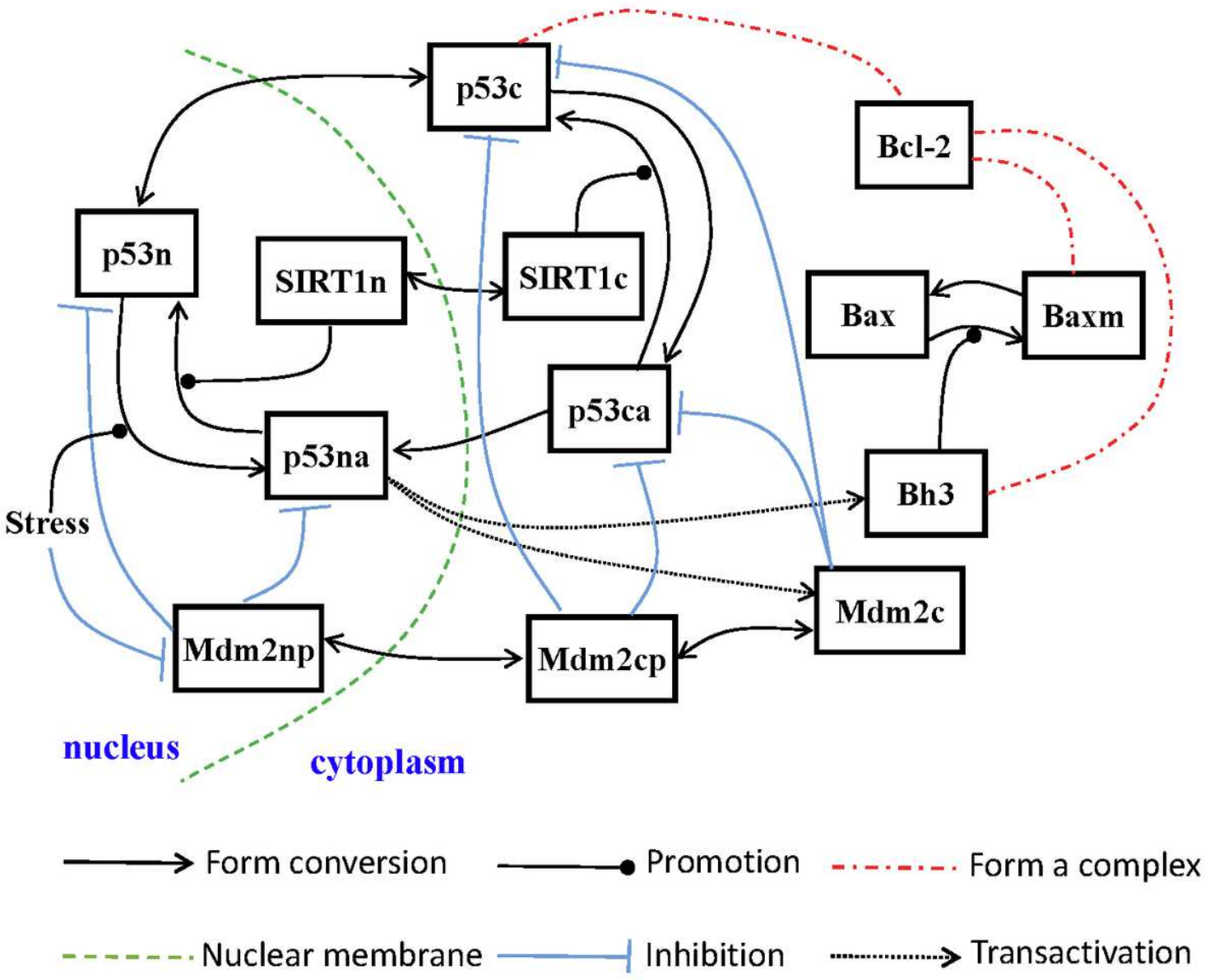

Figure 1

Schematic diagram of the model. Pn and Pc represent the protein P in the nucleus and cytoplasm, respectively; the *a*' and p' at the end of the protein represent acetylation and phosphorylation, respectively; the `m' at the end of the protein represents the protein inlaid on the outer mitochondrial membrane.

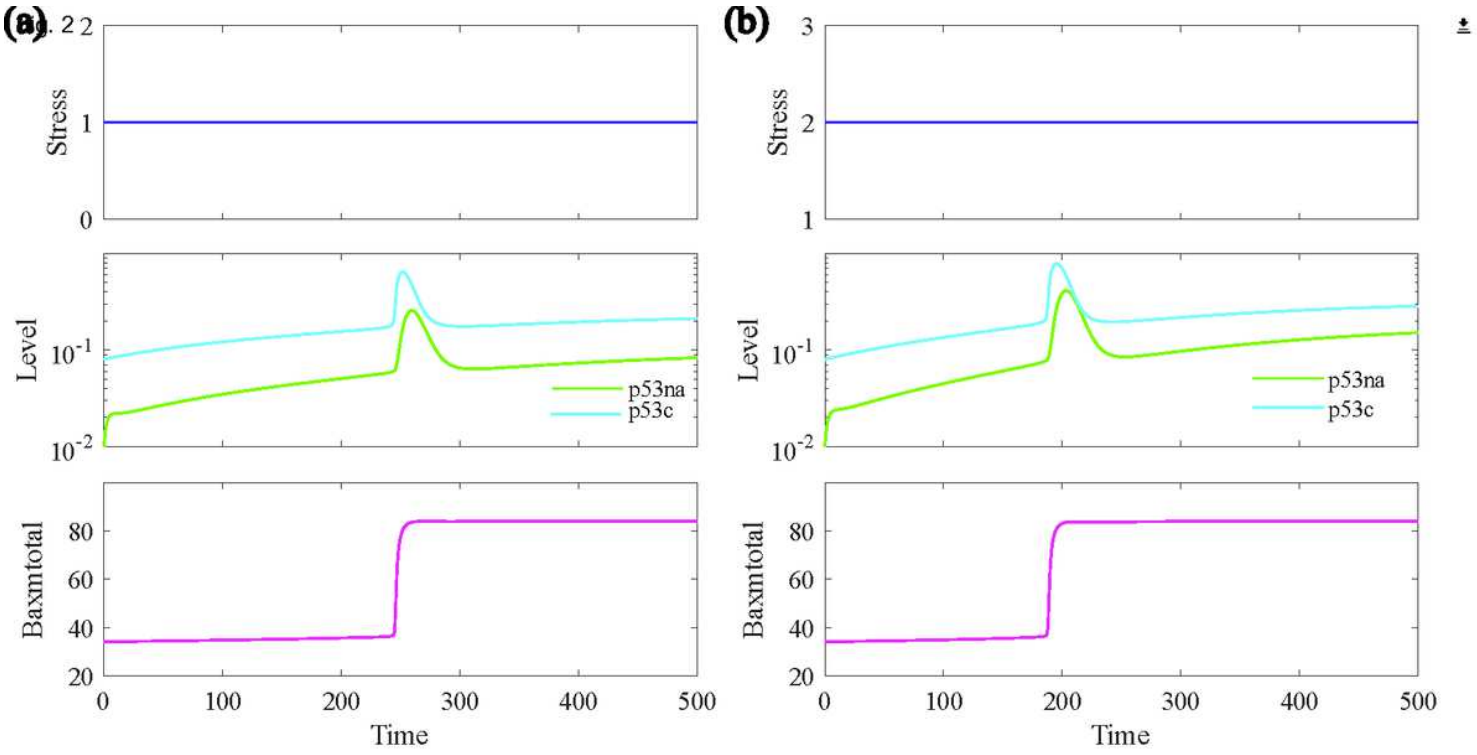

Figure 2

Time courses of stress, p53c, p53na, and Baxmtotal. Here [Stress]0 = 0, and the initial stress=1 in (a), =2 in (b).

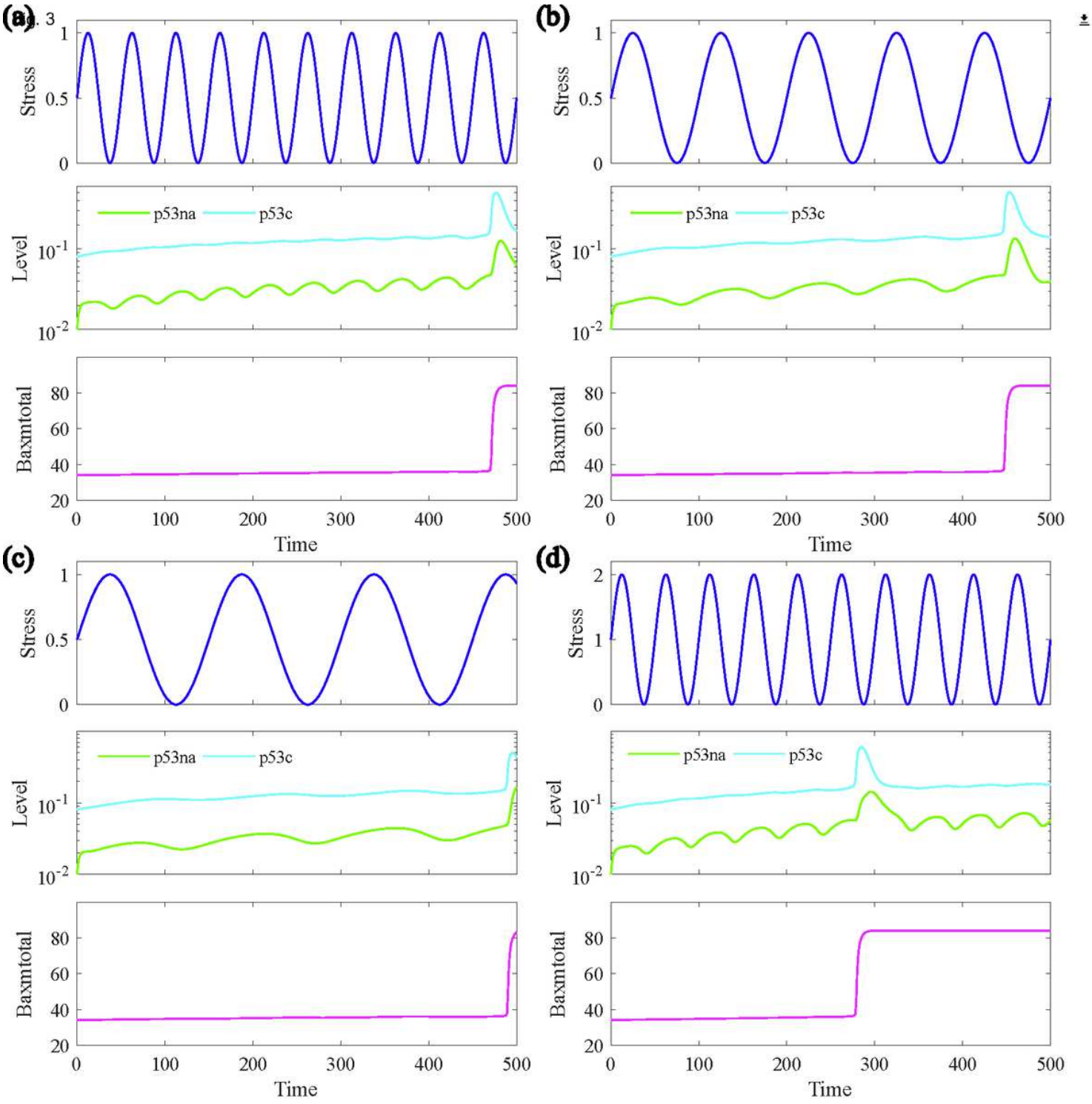

Figure 3

Time courses of stress, p53c, p53na, and Baxmtotal. Here [Stress]0 = Amplitude(2⍰=Period)cos(2⍰t=Period), and the initial stress=0.5 in (a), (b), and (c), =1 in (d); Amplitude=1 in (a), (b), and (c), =2 in (d); Period=50 in (a) and (d), =100 in (b), =150 in (c).

Fig. 4

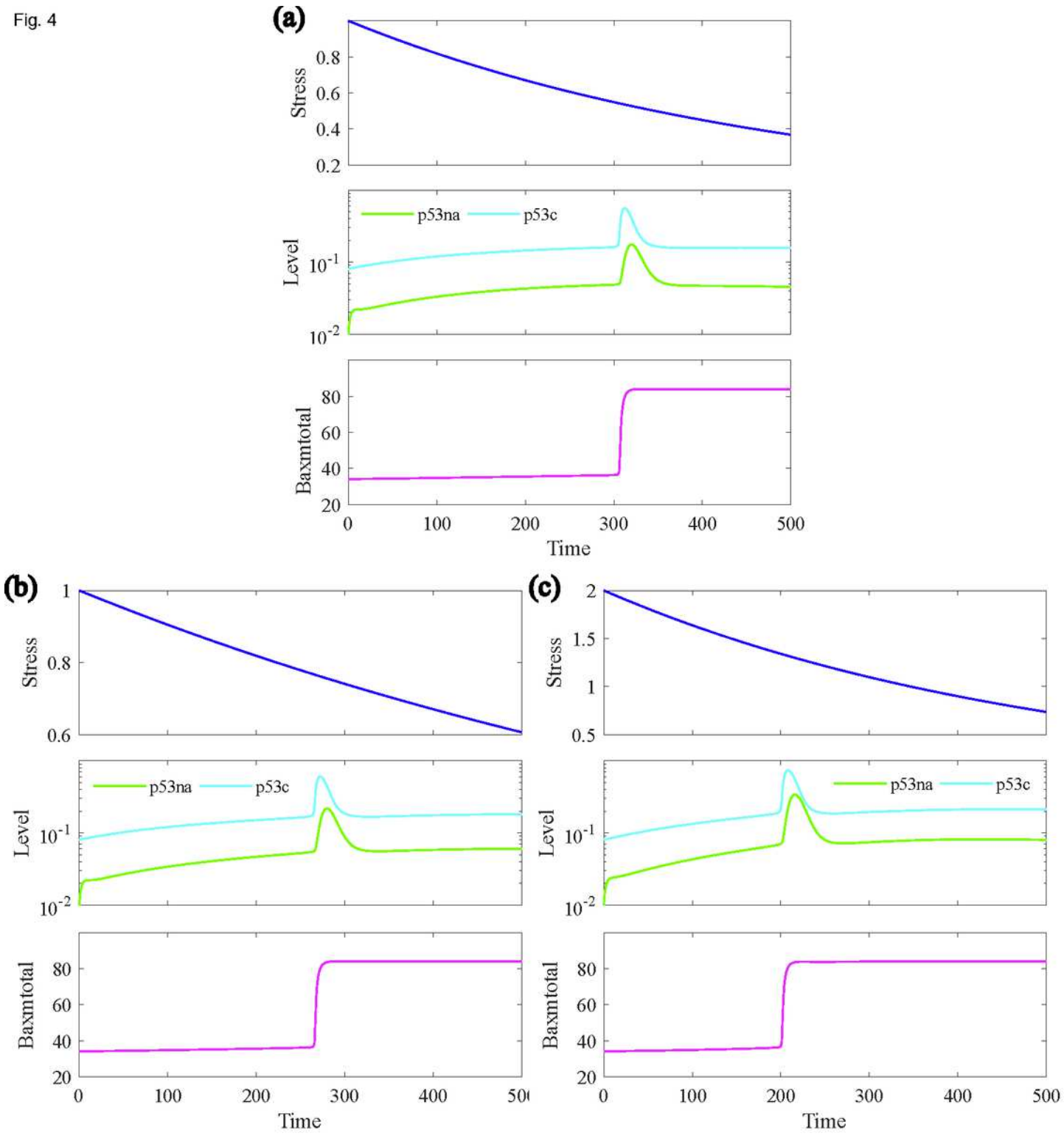

Figure 4

Time courses of stress, p53c, p53na, and Baxmtotal. Here [Stress]0 = □k[Stress], and the initial stress=1 in (a) and (b), =2 in (c); k=0.002 in (a) and (c), =0.001 in (b).

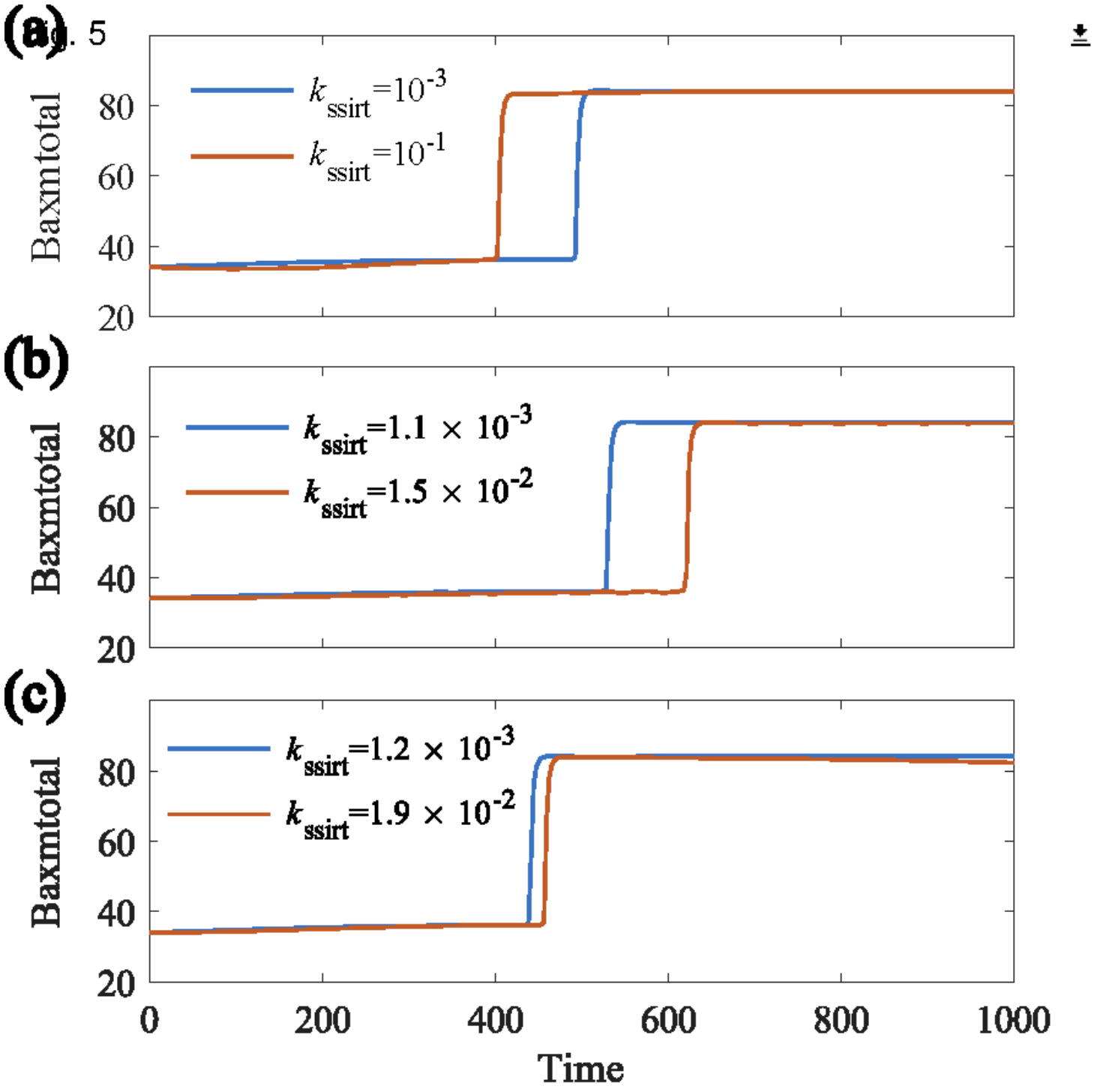

Figure 5

Time courses of stress Baxmtotal. Here kssirt in the cases of the blue lines are less than the default value, and in the cases of the orange lines are greater than the default value. The stress situation of (a) is the same as Fig. 2(a); The stress situation of (b) is the same as Fig. 3(a); And the stress situation of (c) is the same as Fig. 4(a).

Fig. 6

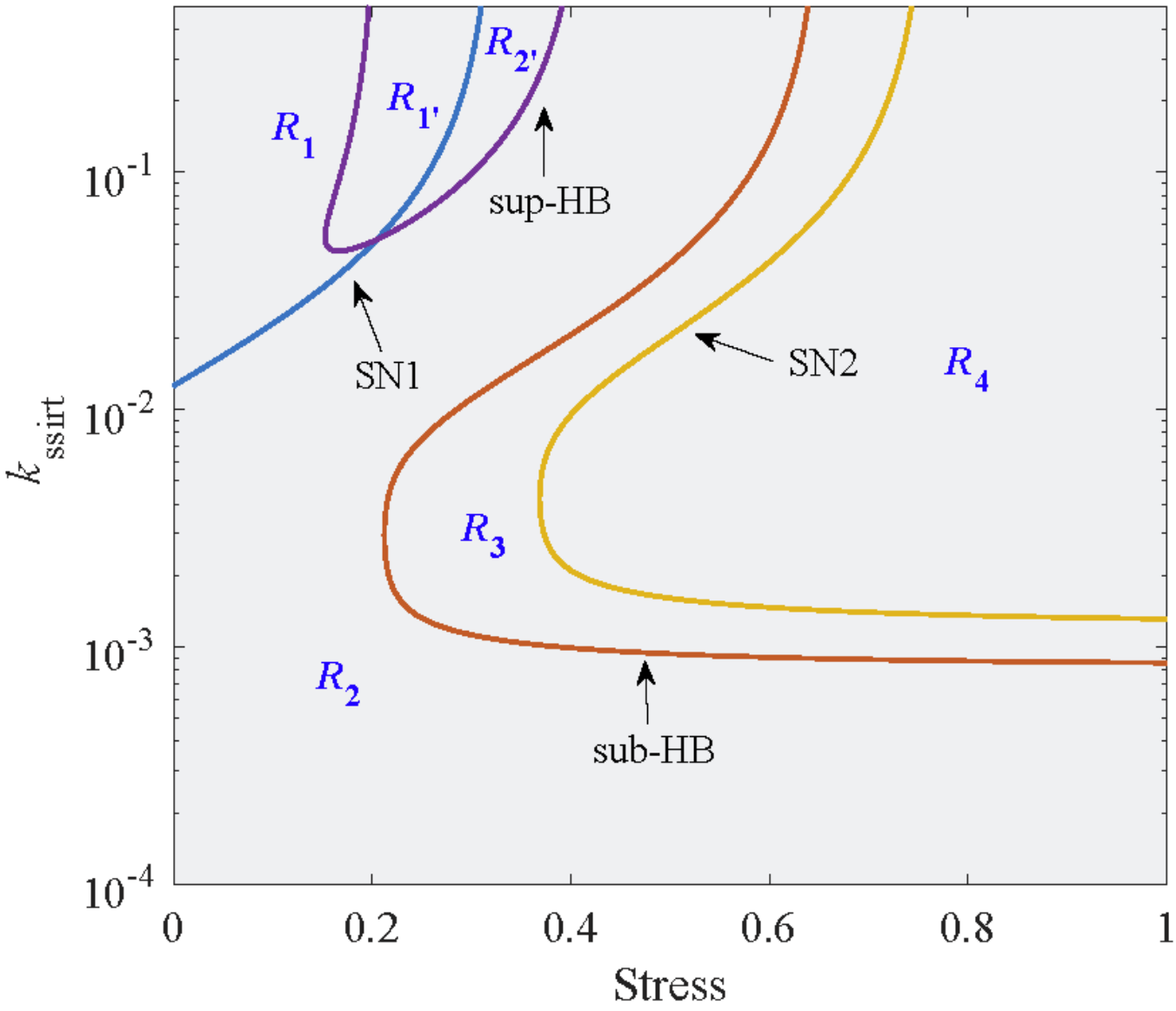

Figure 6

Two-dimensional bifurcation diagram showing various types of bifurcation lines (Stress, kssirt)-plane. The bifurcation lines divide the parameter domain into six subregions. Here SN stands for saddle node bifurcation, sup- or sub-HB stands for supercritical or subcritical Hopf bifurcation.

Fig. 7

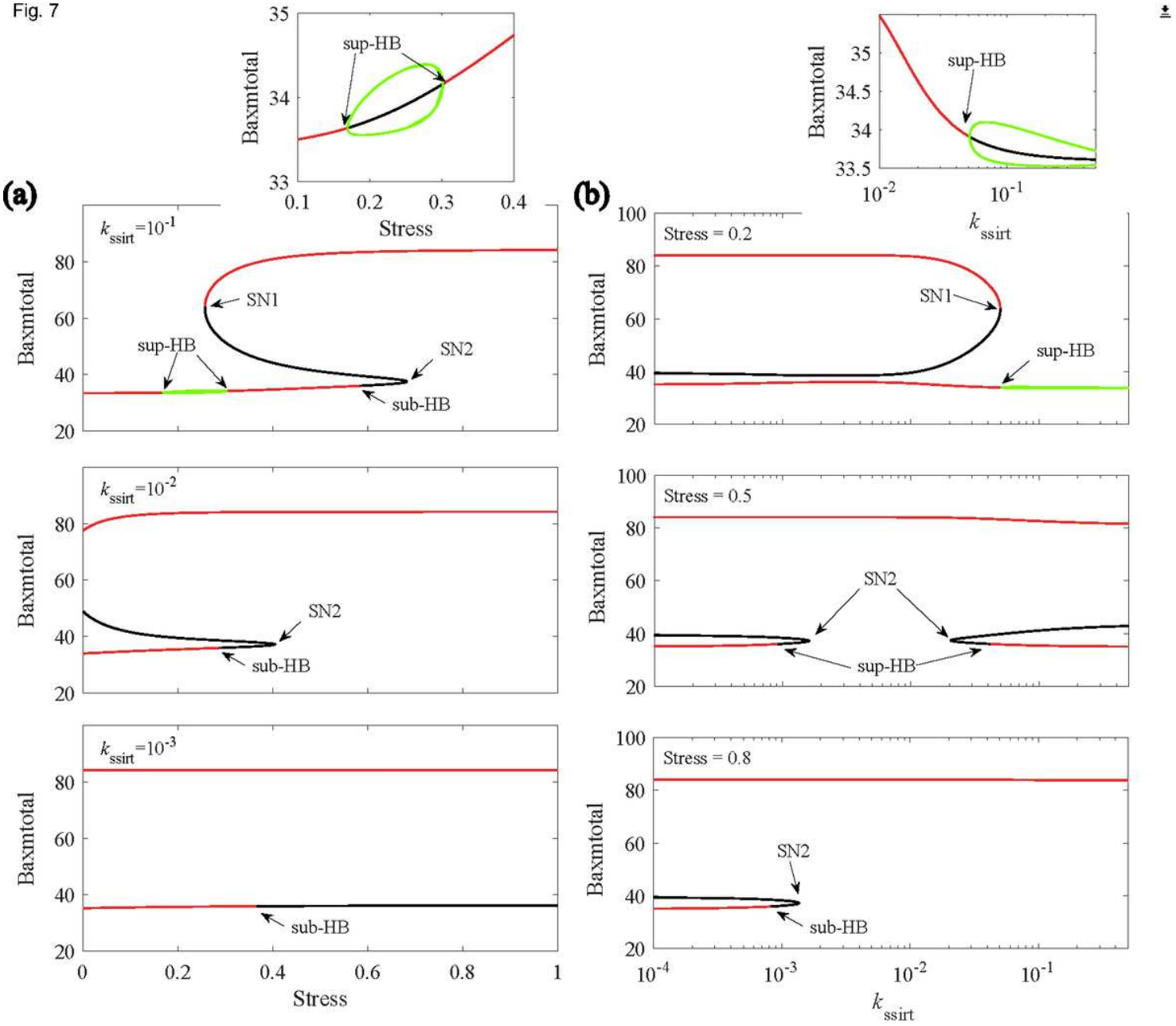

Figure 7

One-dimensional bifurcation diagrams. SN, sup-HB, and sub-HB have the same meaning as Fig. 6. The stable and unstable steady states are indicated by red and black lines, respectively. Green lines are the maxima and minima of the stable limit cycles. The small picture is an enlargement of the oscillation interval.